

# Enhanced Osseointegration of Titanium Implants by Surface Modification with Silicon-doped Titania Nanotubes

This article was published in the following Dove Press journal:  
*International Journal of Nanomedicine*

Xijiang Zhao<sup>1,\*</sup>  
Linna You<sup>1,\*</sup>  
Tao Wang<sup>1</sup>  
Xianjun Zhang<sup>1</sup>  
Zexi Li<sup>2</sup>  
Luguang Ding<sup>2</sup>  
Jiaying Li<sup>2</sup>  
Can Xiao<sup>2</sup>  
Fengxuan Han<sup>2</sup>  
Bin Li<sup>2</sup> 

<sup>1</sup>Department of Orthopedics, The Affiliated Hospital of Jiangnan University, Wuxi, Jiangsu 214062, People's Republic of China; <sup>2</sup>Departments of Orthopaedic Surgery and Stomatology, The First Affiliated Hospital, Orthopaedic Institute, Soochow University, Suzhou, Jiangsu 215006, People's Republic of China

\*These authors contributed equally to this work

Correspondence: Bin Li  
Soochow University (South Campus), 708 Renmin Road, Rm 308 Bldg 1, Suzhou, Jiangsu 215007, People's Republic of China  
Tel/Fax (+86) 512-6778-1163  
Email binli@suda.edu.cn

Can Xiao  
The First Affiliated Hospital of Soochow University, 188 Shizi Street, Suzhou, Jiangsu 215006, People's Republic of China  
Email canxiao0511@163.com

**Introduction:** Despite great progress made in developing orthopedic implants, the development of titanium (Ti) implants with ideal early osseointegration remains a big challenge. Our pilot study has demonstrated that Si-TiO<sub>2</sub> nanotubes on the surface of Ti substrates could enhance their osteogenic activity. Hence, in this study, we aim to comprehensively evaluate the effects of silicon-doped titania (Si-TiO<sub>2</sub>) nanotubes on the osseointegration property of Ti implants.

**Materials and Methods:** The Ti implants were surface modified with Si-TiO<sub>2</sub> nanotubes through in situ anodization and Si plasma immersion ion implantation (PIII) method. Three groups were divided as Ti implants (Ti), Ti modified with TiO<sub>2</sub> nanotubes (TiO<sub>2</sub>-NTs) and Ti modified with Si-TiO<sub>2</sub> nanotubes (Si-TiO<sub>2</sub>-NTs). The morphology of Si-TiO<sub>2</sub> nanotubes was observed by scanning electron microscope. The growth and osteogenic differentiation of MC3T3-E1 cells on the Ti implants were evaluated. Further, the pull-out tests and in vivo osseointegration ability evaluation were performed after implanting the screws in the femur of Sprague Dawley rats.

**Results:** The Si-TiO<sub>2</sub> nanotubes could be seen on the surface of Ti implants. The MC3T3-E1 cells could grow on the surface of Ti, TiO<sub>2</sub>-NTs and Si-TiO<sub>2</sub>-NTs, and showed fast proliferation rate on the Si-TiO<sub>2</sub>-NTs. Moreover, the production of some osteogenesis-related proteins (ALP and Runx2) at one week and calcium deposition at four week was also enhanced in Si-TiO<sub>2</sub>-NTs rather than other groups. In vivo osseointegration results showed that Si-TiO<sub>2</sub> nanotube-modified Ti screws had higher pullout force at two and four weeks as well as enhanced new bone formation at six weeks compared to bare Ti screws and Ti screws modified with TiO<sub>2</sub> nanotubes alone.

**Discussion:** The modification of Si-TiO<sub>2</sub>-NTs on the Ti substrate could generate a nano-structured and hydrophilic surface, which can promote cell growth. Moreover, the existence of the TiO<sub>2</sub> nanotubes and Si element also can improve the in vitro osteogenic differentiation of MC3T3-E1 cells and early bone formation around the implanted screws. Together, findings from this study show that surface modification of Ti implants with Si-TiO<sub>2</sub> nanotubes could enhance early osseointegration and therefore has the potential for clinical applications.

**Keywords:** osseointegration, implant, silicon, titanium dioxide, nanotubes

## Introduction

Titanium (Ti) has been widely used in hard tissue repair such as hip and knee joints due to the high mechanical properties and good biocompatibility.<sup>1</sup> However, in some clinical applications, it is important to achieve faster peri-implant healing. It is believed that optimizing the surface properties of implants can facilitate the adhesion of bone-forming cells and thereby promote early osseointegration.<sup>2-4</sup>

Generally, a thin (2–5 nm) film of titania, or titanium dioxide ( $\text{TiO}_2$ ), forms on the surface of titanium implant, which can protect the titanium substrate from corrosion when it is exposed to air.<sup>5</sup> However, such a  $\text{TiO}_2$  layer does not effectively recruit cells to facilitate bone formation.<sup>6</sup> Therefore, a variety of surface modification techniques including anodization have been used to improve osseointegration.<sup>7,8</sup> For example, well-organized topographic cues at nano/microscales could improve biocompatibility and promote bone formation, which are crucial for successful osseointegration between implant and bone.<sup>9,10</sup> Thus, implants modified with nano-/micro-structured surface, being capable of regulating cell behaviors, are very promising for orthopedic applications.<sup>11</sup> For example, the filopodia of cells can go into the pore of nanotubes to form a locked-in cell structure for bone ingrowth.<sup>12</sup>

In addition, surface chemistry is another aspect to influence the cell/tissue-material interactions.<sup>13</sup> In a recent study, the surface of a clustered  $\text{TiO}_2$  nanotubular structure, fabricated by anodization, was further modified with platelet derived growth factor-BB (PDGF-BB) to enhance expression of osteogenesis-related genes of bone marrow mesenchymal stem cells (BM-MSCs).<sup>14</sup> The incorporation of bioactive elements such as silicon (Si) was conducted to improve the biological performances of biomaterials. The element of Si has been reported to accelerate bone mineralization and enhance the proliferation, differentiation and collagen production of osteoblasts.<sup>15–17</sup> Therefore, Si-incorporated biomaterials including hydroxyapatite,<sup>18,19</sup> tricalcium phosphate<sup>20,21</sup> and polymer scaffold<sup>22,23</sup> have been applied to stimulate bone growth and bone healing. Moreover, our pilot work also demonstrated that Si- $\text{TiO}_2$  nanotubes on the surface of Ti substrates could enhance their biocompatibility and osteogenic activity.<sup>24,25</sup> However, the *in vivo* osseointegration was not comprehensively evaluated in our previous studies.

Therefore, in this study, the Ti screws were surface modified with Si- $\text{TiO}_2$  nanotubes through *in situ* anodization and Si plasma immersion ion implantation (PIII), which is a versatile process and commonly used for the surface modification. To confirm the effects of the nanotubular structures and biochemical cues on osteogenic activity of Ti implants, both *in vitro* cell, and *in vivo* animal experiments were conducted. Accordingly, three kinds of samples, pure Ti implant (termed as Ti group), Ti implant surface modified with  $\text{TiO}_2$  nanotubes ( $\text{TiO}_2$ -

NTs group) or Si- $\text{TiO}_2$  nanotubes (Si- $\text{TiO}_2$ -NTs group) were prepared.

## Materials and Methods

### Sample Preparation

Commercial pure Ti discs with the same thickness (1 mm) and different diameter (5.8 mm, 13 mm and 31 mm) were used for the *in vitro* experiment (Cp Ti, TA1, purity >99.85%). For *in vivo* experiments, pure Ti screws with a length of 10 mm, outer thread diameter of 2.0 mm, inner thread diameter of 1.7 mm were employed. These titanium-based materials were supplied by Tianjin Zhengtian Medical Device Company. Disk samples were polished to a near mirror finish and ultrasonically cleaned in acetone, ethanol and ultra-pure water prior to use.  $\text{TiO}_2$ -NTs samples were prepared by anodization according to the method described in our previous work.<sup>26</sup>

Then, Si- $\text{TiO}_2$ -NTs were produced by Si-PIII with a filtered cathodic arc plasma source.<sup>24,25</sup> In brief, the 99.99% pure silicon rods were used as the cathode. During Si-PIII, a negative pulse voltage of 20 kV was applied, the main arc current and pulsed high voltage applied to target was synchronized at a pulsing frequency of 8 Hz. The pulse duration of the high voltage was 450 ms the same as the pulse duration of the cathodic arc current. The chamber pressure was  $4.0 \times 10^{-3}$  Pa, and the temperature of sample stage was kept at approximately 25°C by circulating water.

### Surface Characterizations

The surface morphologies of the samples before and after PIII were examined by scanning electron microscopy (SEM, S3400, Hitachi, Japan). The surface wettability was assessed using a contact angle instrument (SL200B, Solon, China) according to previous works.<sup>27</sup>

### Cell Culture

MC3T3-E1 mouse pre-osteoblasts (CRL-2594, subclone 14, ATCC) were cultured in alpha minimum essential medium ( $\alpha$ -MEM, Gibco) with 10% FBS (Gibco) and 1% penicillin/streptomycin under 37°C, five percent  $\text{CO}_2$  environment. The Ti,  $\text{TiO}_2$ -NTs and Si- $\text{TiO}_2$ -NTs with the diameter of 5.8 mm were placed in 96-well tissue culture plates, and the density of the cells initially seeded was  $1 \times 10^4$  cells/well. The Ti,  $\text{TiO}_2$ -NTs and Si- $\text{TiO}_2$ -NTs discs ( $\Phi$ , 13 mm) were placed on 24-well plates and the cell density was  $3 \times 10^4$  cells/well. The Ti,  $\text{TiO}_2$ -NTs and Si-

TiO<sub>2</sub>-NTs discs ( $\Phi$ , 31 mm) were placed on six-well polystyrene plates and the cell density was  $3 \times 10^5$  cells/well. In the osteogenic differentiation assay, after the cells were cultured for 24 h, 10 mM  $\beta$ -glycerol phosphate, 50  $\mu$ g/mL ascorbic acid, and 10 nM dexamethasone were added in the medium as the osteogenic induction medium. The cultured media were refreshed every three days.

## Cell Morphology

The MC3T3-E1 cells were seeded on Ti, TiO<sub>2</sub>-NTs and Si-TiO<sub>2</sub>-NTs ( $\Phi$ , 5.8 mm), respectively, for observing cell morphology. After culturing cells for one, three, and five days, the samples were washed twice with PBS and fixed with 2.5 % glutaraldehyde (Sigma, USA) in PBS for one hour. After rinsing three times with PBS for 10 min, the samples were dehydrated in a graded series of ethanol (30%, 50%, 70%, 90%, and 100%) for 30 min each. The samples were dried through a CPD030 Critical Point Dryer (Leica Microsystems, Germany) and sputter-coated with a gold layer using a Hitachi E-1010 Ion Sputter (Quorum Technologies, Laughton, East Sussex UK). Finally, the morphology of cells was observed by SEM (Quanta, USA).

## MTS Assay

The MC3T3-E1 cells were seeded on Ti, TiO<sub>2</sub>-NTs and Si-TiO<sub>2</sub>-NTs ( $\Phi$ , 5.8 mm) for MTS assay. After cell culture for one, three, and five days, the samples were washed three times with PBS to eliminate nonviable cells and transferred to a new 96-well plate for analyzing those cells on the surface of Ti substrates. Then 100  $\mu$ L of culture medium and 20  $\mu$ L of MTS reagent (Promega, USA) were added to each well following the manufacturer's directions. After incubating for two hours, the absorbance of each solution was measured at a wavelength of 490 nm using a 96-well plate reader on a spectrophotometer (Spectrophotometer U-3010, Hitachi, Japan).

## Calcium Deposition

After seeding MC3T3-E1 cells and subsequent osteogenic induction culture, the extracellular matrix (ECM) mineralization of cells on the samples was evaluated by alizarin red (Sigma) staining. After osteogenic induction for three and four weeks, the Ti, TiO<sub>2</sub>-NTs and Si-TiO<sub>2</sub>-NTs samples ( $\Phi$ , 13 mm) were fixed in 75% ethanol for one hour. Then, cells were rinsed with double-distilled water and stained 200  $\mu$ L of 40 mM alizarin red S solution (pH 4.1) for 10 min at room temperature. Afterwards, the

unbound stain was washed with distilled water before the images were taken. In the quantitative analysis, the stained samples were dissolved with 0.5 M HCl-5% sodium dodecyl sulphate (SDS) solution for 30 min at room temperature.<sup>28</sup> Then, the absorbance of the solution was determined at 405 nm on a spectrophotometer (Spectrophotometer U-3010, Hitachi, Japan).

## Western Blot Analysis

The MC3T3-E1 cells cultured on Ti, TiO<sub>2</sub>-NTs and Si-TiO<sub>2</sub>-NTs ( $\Phi$ , 31 mm) were harvested at weeks one, two, and three, respectively. Thirty micrograms of cell lysate were separated by 12% SDS-PAGE gels and transferred to nitrocellulose membranes. After blocking in specific monoclonal anti- $\beta$ -actin (ab3280) primary antibodies (Abcam Biotechnology) HRP conjugated immunoglobulin was used as the secondary antibody (Jackson ImmunoResearch Laboratories). Then, West Pico Chemiluminescent (Pierce) was adopted as the substrate to visualize protein bands, which were quantified using densitometry image analysis software (Image Master VDS, Pharmacia Biotech). Normalization was made against  $\beta$ -actin expression.

## In vivo Osseointegration Study Surgical Implantation

All the animal experiments were approved by the Institutional Animal Care and Use Committee (IACUC) of Soochow University, and all procedures followed the NIH guidelines for the care and use of laboratory animals. Thirty-six male Sprague Dawley rats (260–280 g weight) supplied by Soochow University Animal Center were used for the animal experiment. Among them, 27 rats were used for mechanical tests and nine rats for micro-CT and histological analysis. Implantations were divided into three groups as follows: Ti (pure Ti screws), TiO<sub>2</sub>-NTs (Ti screws modified by TiO<sub>2</sub> nanotubes), and Si-TiO<sub>2</sub>-NTs (Ti screws modified by Si-TiO<sub>2</sub> nanotubes). Systemic anesthesia injection was adopted using ketamine and xylazine at 80–100 mg/kg and 10–20 mg/kg, respectively. Additional local anesthesia was also performed in the surgery field with 2% lidocaine solution containing epinephrine (1:100,000). The hair of surgical site was removed and sterilized with betadine scrubs. Flat surface of the distal femur was selected for implant placement. The screws were implanted from the outside to the inside in the horizontal direction. Each rat received one implant (Ti, TiO<sub>2</sub>-NTs or Si-TiO<sub>2</sub>-NTs) in each femur. At the tenth and third day before sacrifice, the animals received

subcutaneous injections of fluorochrome label (calcein). The experimental animals were sacrificed at the time by an intraperitoneal excessive dose of sodium pentobarbital.

### Mechanical Tests

Three rats of each group were sacrificed at two, four, and six weeks after surgery. Pull-out tests were performed for all implants (six samples per group) in the femur. The femurs were mounted in the machine with the head of the screw pointing out of a hole in a metal book holder (Figure 1). The screws were tested for pull-out strength using a mechanical testing machine (HY-1080, Shanghai, China). A load cell (maximum force of 500 N) at a test speed of 1 mm/min was applied. The maximal force during the pull-out experiment was considered as the pull-out force.

### Micro-CT and Histological Analysis

After six weeks, the nine rats were sacrificed and each group had six samples for micro-CT analysis. The bone-screw interface and trabecular microstructure of specimens

were scanned on a micro-CT system (18  $\mu$ m voxel size, 80 kV, 300  $\mu$ A, 290 min exposure time, Cu and Al filter, 0.7° rotation step; SkyScan1176 In vivo Micro-CT, Brüker, Kontich, Belgium). Multilevel thresholding procedures (threshold for bone=75, threshold for implant=115) were applied to discriminate bone from other tissue. The volume of interest (VOI) included the trabecular compartment extending 1.4 mm from the longitudinal axis of the screw.

After micro-CT scan, the distal femurs with screws were prepared for undecalcified histologic sections, each group had six samples for histological analysis. All implant sites were processed through gradient ethanol dehydration and xylene substitute before being infiltrated and embedded in methyl methacrylate to individually labeled blocks.

### Statistical Analysis

Quantitative data were expressed as the mean  $\pm$ SD. Statistical analysis was performed with unpaired

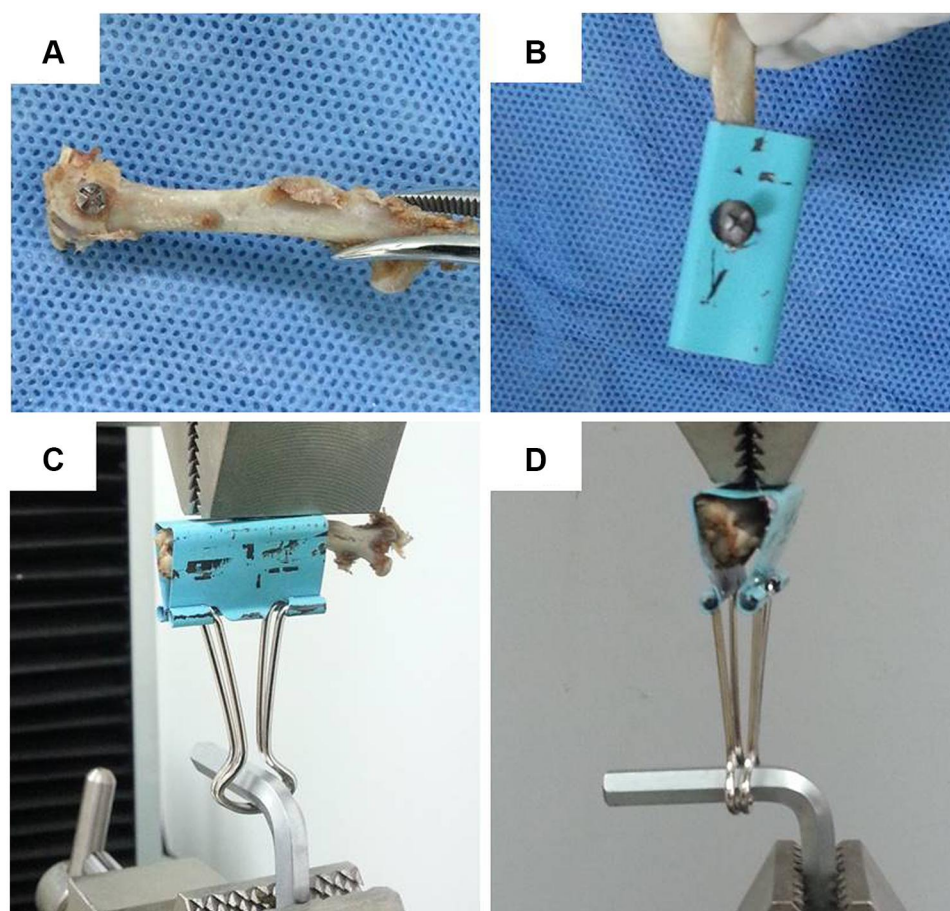


**Figure 1** Experimental set-up for pull-out analyses: (A) The position of screw at the distal femur, and (B–D) show the mounted femur in the material testing machine.

two-tailed Student's *t*-test for single comparisons with SPSS 18.0 (SPSS Inc., Chicago, IL, USA). ANOVA was used to compare data from more than two groups. A value of  $p < 0.05$  denotes statistically significant difference.

## Results

### Surface Properties of Modified Ti Substrates

Figure 2A and B show the SEM images of TiO<sub>2</sub>-NTs and Si-TiO<sub>2</sub>-NTs. After anodization, the surface of titanium substrate showed a regular tubular nanostructure, and the outer and inner diameter of these nanotubes are about 80 nm and 60 nm, respectively (Figure 2A and B). Treated by Si-PHII, the nanotubular structures could still be observed but some pores are enclosed. The water contact angles of Si-TiO<sub>2</sub>-NTs, TiO<sub>2</sub>-NTs and pure Ti are  $11.25 \pm 0.88^\circ$ ,  $35.89 \pm 1.38^\circ$  and  $65.14 \pm 4.05^\circ$ , respectively (Figure 2CE). The results indicate that Si-TiO<sub>2</sub>-NTs were more hydrophilic than TiO<sub>2</sub>-NTs and Ti.

### Cell Morphology

Cell morphology on Ti, TiO<sub>2</sub>-NTs and Si-TiO<sub>2</sub>-NTs at one, three, and five days was observed by SEM, as shown in Figure 3. After one day of cultivation, cells on the Ti show a flattened morphology, meanwhile the cells on TiO<sub>2</sub>-NTs and Si-TiO<sub>2</sub>-NTs are round and irregular shape. Moreover, finger-like filopodia extensions could be observed on the Si-TiO<sub>2</sub>-NTs. At day three, the cells on the Ti and TiO<sub>2</sub>-NTs exhibit

elongated and flattened morphology. Filopodia extensions could also be observed on the Si-TiO<sub>2</sub>-NTs, on which cells begin to merge. At day five, all the groups are covered with cells. Much more mesh-like filopodia appear on TiO<sub>2</sub>-NTs than Ti, while many filamentous network structures with excellent intercellular attachment could be found on Si-TiO<sub>2</sub>-NTs.

### Cell Proliferation

Figure 4A shows the MTS assay result of cells cultured on Ti, TiO<sub>2</sub>-NTs and Si-TiO<sub>2</sub>-NTs for one, three and five days. The cells on all samples proliferate gradually. After one and three days of incubation, cell proliferation on substrate with nanotubular surfaces is higher than that on Ti, and there is no significant difference between Si-TiO<sub>2</sub>-NTs and TiO<sub>2</sub>-NTs. At day five, cells on Si-TiO<sub>2</sub>-NTs were more than on TiO<sub>2</sub>-NTs, indicating that cell proliferation is enhanced after Si incorporation.

### Calcium Deposition

The results of extracellular matrix mineralization of the MC3T3-E1 cells cultured on three samples are shown in Figure 4B. Compared to Ti, cells on TiO<sub>2</sub>-NTs and Si-TiO<sub>2</sub>-NTs show more calcium mineral nodule formation both at three and four weeks. Moreover, the amount of deposited calcium mineral on Si-incorporated samples is higher than those on TiO<sub>2</sub>-NTs at four weeks.

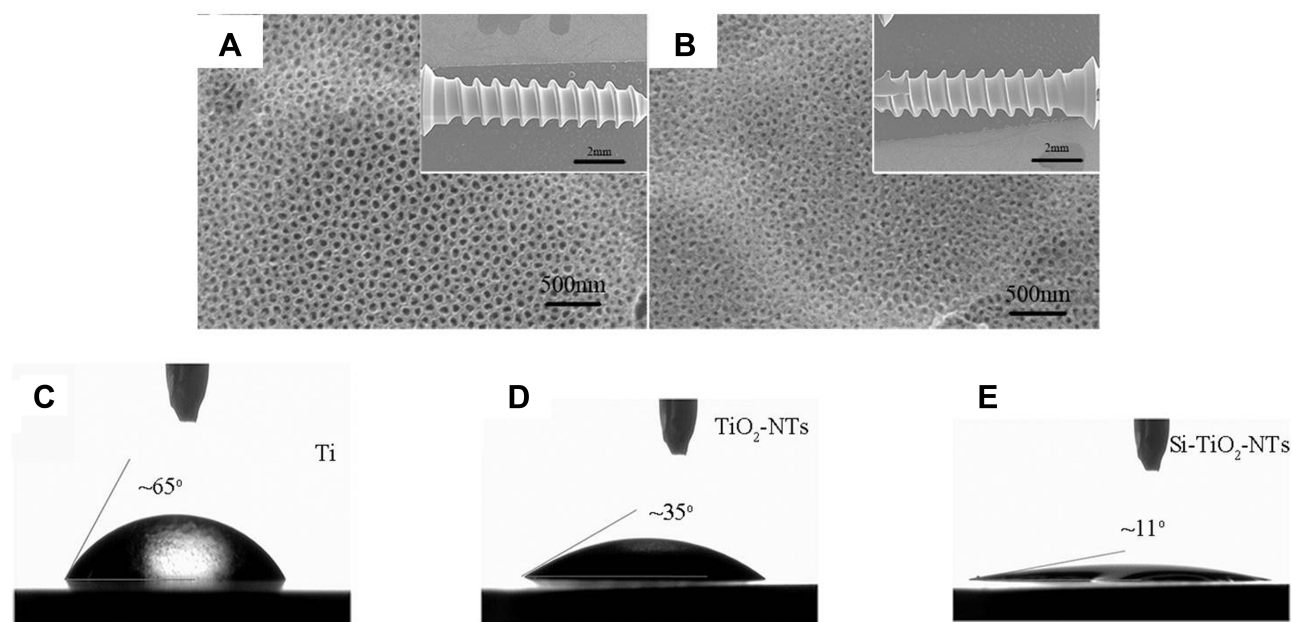
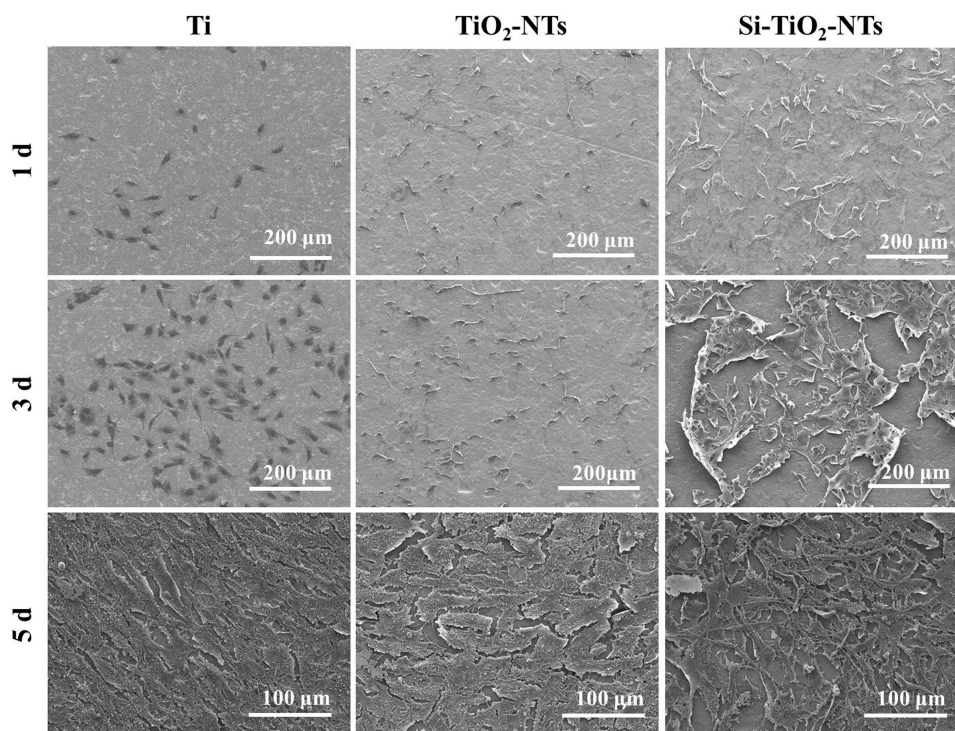
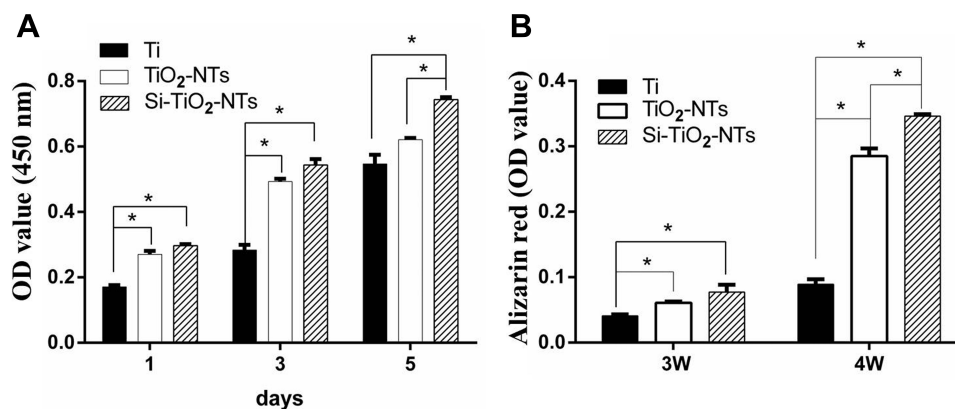


Figure 2 SEM images of the TiO<sub>2</sub>-NTs (A) and Si-TiO<sub>2</sub>-NTs (B) screws, and water contact angles of Ti (C), TiO<sub>2</sub>-NTs (D) and Si-TiO<sub>2</sub>-NTs (E).



**Figure 3** Morphology of MC3T3-E1 cultured on Ti, TiO<sub>2</sub>-NTs and Si-TiO<sub>2</sub>-NTs for one, three, and five days, respectively.



**Figure 4** Cell viability and proliferation (A) shown by MTS assay of MC3T3-E1 cells cultured on Ti, TiO<sub>2</sub>-NTs and Si-TiO<sub>2</sub>-NTs for one, three, and five days, and calcium deposition determined (B) by alizarin red staining for -three and four weeks. \**p*<0.05.

## Western Blot

The results of Western blotting analysis are shown in Figure 5. The expressions of Runx2, ALP and Col-I of cells cultured on the three samples are presented and β-actin was adopted as control (Figure 5A). The quantitative results of proteins expression are also displayed in Figure 5B. An enhanced expression of Runx2 is observed on Si-TiO<sub>2</sub>-NTs compared to TiO<sub>2</sub>-NTs and Ti at weeks one and three. The levels of ALP expression are obviously increased on Si-TiO<sub>2</sub>-NTs rather than TiO<sub>2</sub>-NTs at week

one. The protein expression of Col-I does not show significant difference among these samples.

## In vivo Osseointegration

### Pull-out Force Measurement

As shown in Figure 6, the pull-out force of TiO<sub>2</sub>-NTs is significantly higher than Ti. Moreover, the Si-TiO<sub>2</sub>-NTs group exhibits the highest pull-out force at two and four weeks. The peak pull-out forces increased approximately 18% and 21% on Si-implanted samples than

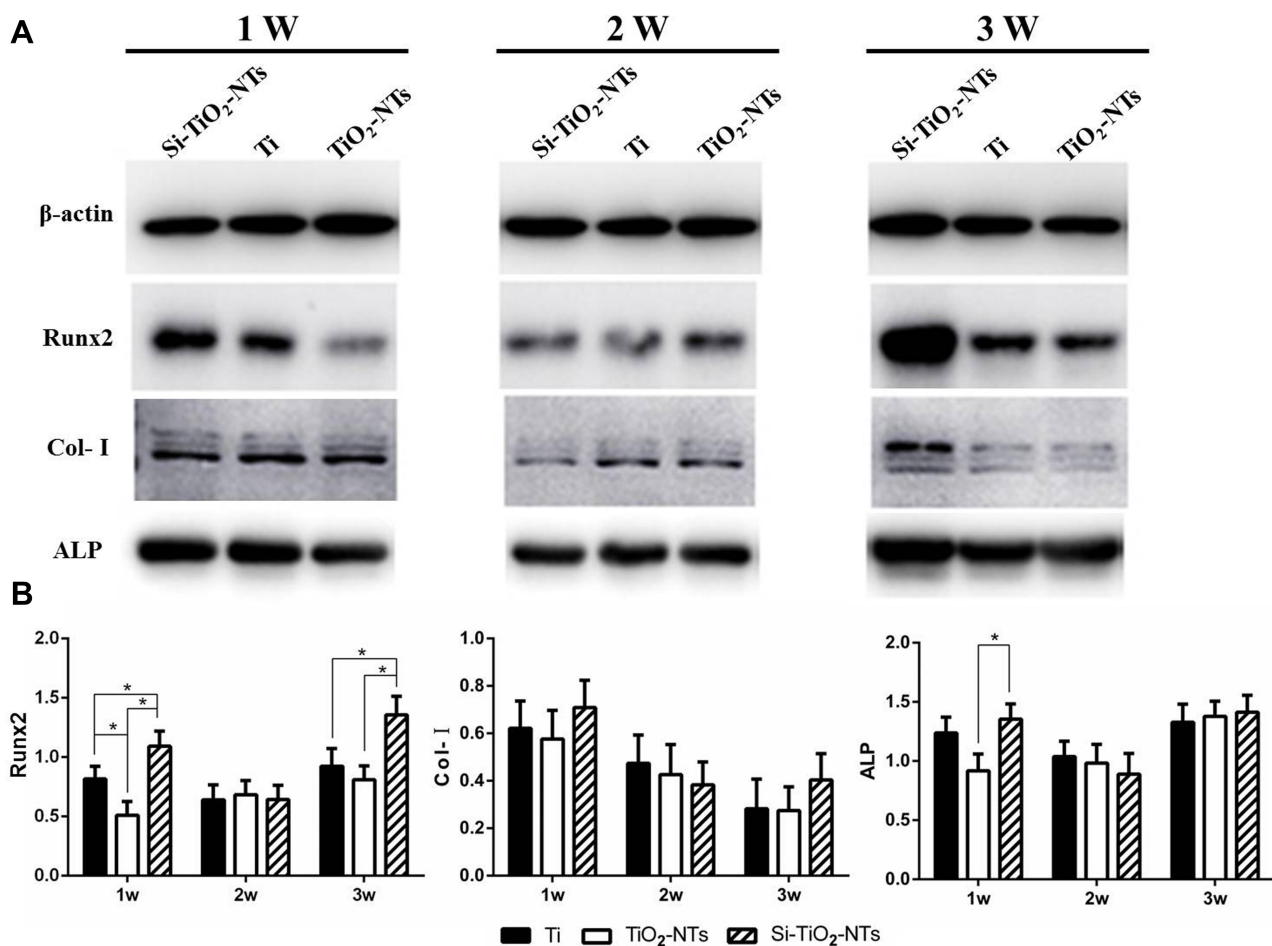


**Figure 5 (A)** Protein expression of Runx2, Collagen I and ALP of MC3T3-E1 cells cultured on Ti, TiO<sub>2</sub>-NTs and Si-TiO<sub>2</sub>-NTs determined by Western blot, β-actin was used as the control, and **(B)** are the corresponding relative intensity. \**p*<0.05.

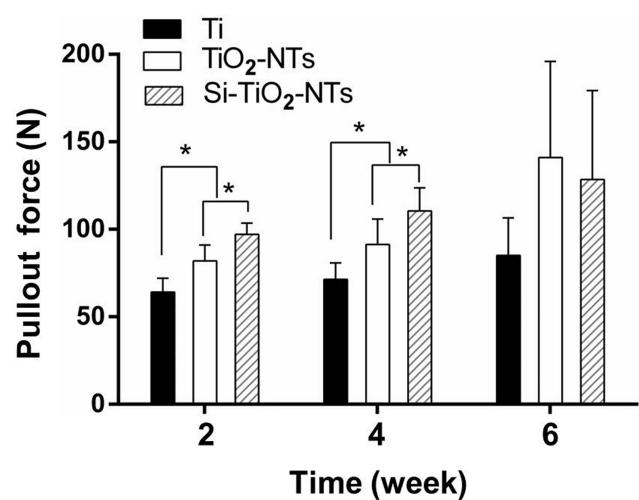


**Figure 6** Pullout forces of screws removal after implantation in rat femurs. \**p*<0.05.

TiO<sub>2</sub>-NTs at weeks two and four, respectively. At week six, there was no significant difference among the three samples.

### Micro-CT and Histological Evaluations

The results of micro-CT six weeks after surgery are shown in [Figure 7](#). From the two-dimensional micro-CT images, more cancellous bone is observed around the Si-TiO<sub>2</sub>-NTs screws than the controls ([Figure 7A](#)). Quantitative evaluation is presented in [Figure 7B](#), and more detailed information is obtained on percentage osteointegration (% OI) and trabecular parameters around screws. Compared to Ti screws, the % OI of Si-TiO<sub>2</sub>-NTs and TiO<sub>2</sub>-NTs increases to 65% and 54%, respectively. The bone volume ratio (BV/TV) values of Si-TiO<sub>2</sub>-NTs and TiO<sub>2</sub>-NTs are about 4.2-fold and 2.4-fold than that of Ti. In addition, the trabecular thickness (Tb.Th), trabecular number (Tb.N) and trabecular separation (Tb.Sp) of Si-TiO<sub>2</sub>-NTs and TiO<sub>2</sub>-NTs are all higher than that of Ti.

The histological images are displayed in [Figure 8](#). The fluorochrome labels reflect the different patterns of bone neoformation and remodeling in three groups. Extensive bone apposition could be found between the screw threads at the spongy level on the Si-TiO<sub>2</sub>-NTs and TiO<sub>2</sub>-NTs.

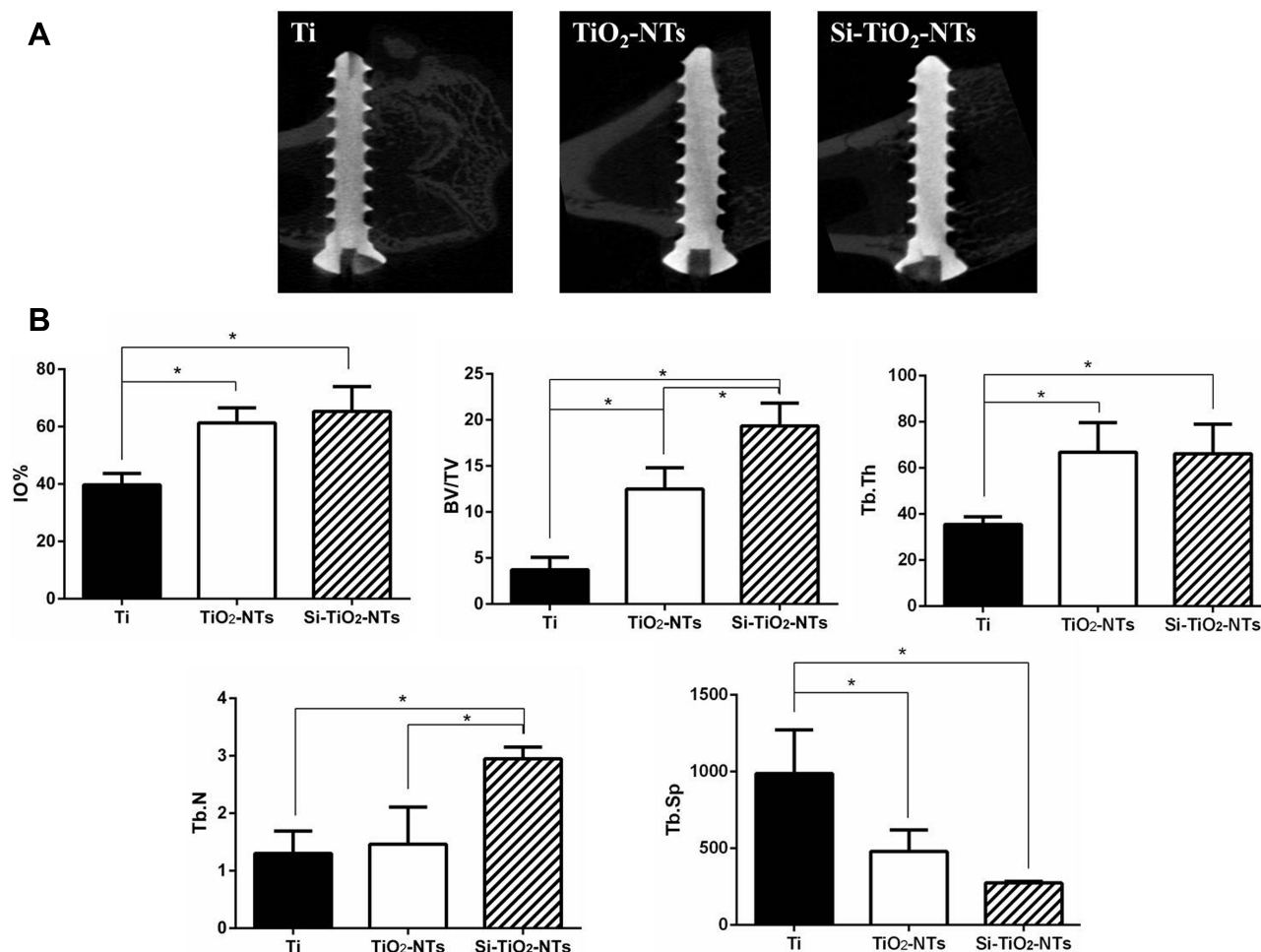


**Figure 7 (A)** The 2D micro-CT images of the sections along the plane of femurs, and **(B)** histograms of percentage osseointegration and trabecular parameters within volume of interest. \* $p < 0.05$ .

**Abbreviations:** % OI, percentage osseointegration; BV/TV, trabecular bone volume density; Tb.Th, trabecular thickness; Tb.N, trabecular number; Tb.Sp, trabecular separation.

And more bone is observed at the internal part of the Si-TiO<sub>2</sub>-NTs screw compared to TiO<sub>2</sub>-NTs, indicating a new bone trabecular formation on the surface of Si-TiO<sub>2</sub>-NTs screw.

## Discussion

Due to the nature of bio-inertness, titanium-based implants can lead to capsule formation after hip or knee replacement surgery and the bone bonding tends to become loose over the long term.<sup>29</sup> Thus, surface modifications are essential for titanium-based implants to achieve better and more rapid bonding to bone. Surface topography<sup>30</sup> and surface chemical compositions,<sup>31</sup> the two major factors, can affect the interactions between implants and cells/tissues. In this work, titanium screws surface-modified with Si-TiO<sub>2</sub> nanotubes were produced and their osteogenesis potential was investigated. Further, titanium screws

and titanium screws surface-modified with TiO<sub>2</sub> nanotubes were adopted as the controls, it may help to understand the roles of nanostructured surface and incorporation of silicon in regulating osteogenesis.

Si was incorporated into the TiO<sub>2</sub> nanotubes on the surface of Ti screws using Si-PHII technique described in our previous studies.<sup>24,25</sup> With this method, Si could be successfully incorporated into TiO<sub>2</sub>-NTs.<sup>25</sup> After Si-PHII treatment, a nanotubular surface was obtained (Figure 2A and B). According to the results of water contact angle, the surface wettability of TiO<sub>2</sub>-NTs is better than pure Ti (Figure 2C and D), which could be attributed to the existence of TiO<sub>2</sub> nanotubes on the surface of Ti screws.<sup>19</sup> Further, it is found that a more hydrophilic surface was obtained after Si incorporation. Another study has demonstrated that the existence of Ti-O-Si on the surface of Si-TiO<sub>2</sub> could improve the hydrophilicity and the capability



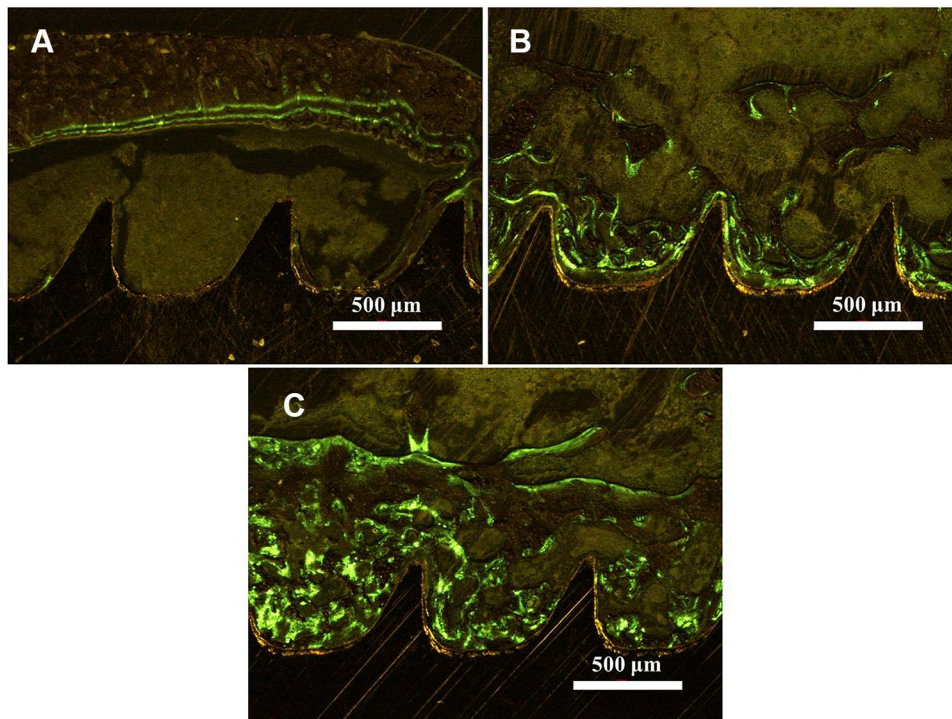


**Figure 8** Histological appearance of Ti (A), TiO<sub>2</sub>-NTs (B) and Si-TiO<sub>2</sub>-NTs (C) samples after six weeks of implantation, Green (calcein) lines are presented as the new bone around the screw. Scale bars, 500 μm.

to hold absorbed water compared to TiO<sub>2</sub> film.<sup>32</sup> In our current study, Ti-O-Si also existed on the surface of Si-TiO<sub>2</sub>-NTs, resulting in the better hydrophilicity of Si-TiO<sub>2</sub>-NTs compared with TiO<sub>2</sub>-NTs. Moreover, our previous study also found that the hydrophilicity of the Ti substrates increases with the incorporated Si amount.<sup>24</sup>

The adhesion of cells on implant surfaces is the first stage after *in vivo* implantation, which defines the quality of the bone bonding.<sup>33</sup> When the cells were cultured on the samples for one, three, and five days, the cells were observed with good adhesion on TiO<sub>2</sub>-NTs than Ti, which may be attributed to the nanostructures on the surface (Figure 3). Oh et al had pointed out that the tubular structures could improve cell adhesion by generating an interlocked structure when cell filopodia went into the pores.<sup>12</sup> Moreover, the cells on the Si-TiO<sub>2</sub> nanotubes showed the best filopodia activities, which may be attributed to the nanostructures and hydrophilic surface. Furthermore, the proliferation of cells was studied by MTS test for one, three, and five days (Figure 4A). Improved cell proliferation was observed on the samples with nanotubular structures. Interestingly, cell proliferation appeared faster at day five on Si-TiO<sub>2</sub>-NTs than on TiO<sub>2</sub>-NTs, which may be related to the Si incorporation. A recent study also demonstrated the potential of Si-

contained biomaterials for patterned cell culture *in vitro*.<sup>34</sup> Other research groups had reported that the existence of Si could improve the metabolism, synthetic activity and osteogenic activity of the cells.<sup>17,35</sup>

To further verify the enhancement of Si on osteogenic activity, the matrix mineralization was investigated by alizarin red S staining (Figure 4B). As a marker of osteogenic activity, the matrix mineralization of TiO<sub>2</sub>-NTs was more than Ti without this surface microstructure. The incorporation of Si in TiO<sub>2</sub>-NTs further enhanced matrix mineralization (Figure 4B). This result showed that the existence of Si and TiO<sub>2</sub> nanotubes could promote osteogenic activity. Although the expression of osteogenesis-related genes was not detected in this study, in our previous study these genes were observed upregulated.<sup>24</sup> In this study, we further determined the expression of osteogenesis-related proteins by Western blotting analysis. Runx2 and ALP, which are early markers for osteogenic differentiation, have been widely used to investigate osteogenic activity.<sup>36,37</sup> Both the expression of Runx2 and ALP increased on Si-TiO<sub>2</sub>-NTs than Ti and TiO<sub>2</sub>-NTs (Figure 5). Increased expression of Runx2 occurred at weeks one and three, and ALP at week one. Moreover, Col-I is the main content of bone ECM, its expression was higher on Si-TiO<sub>2</sub>-NTs although there is no significant difference

among the three samples. Comparing the results of these three groups, it was found that the existence of Si and TiO<sub>2</sub> nanotubes exhibited the highest osteogenic activity in vitro. These findings are consistent with previous studies, in which Si incorporated TiO<sub>2</sub> on titanium showed enhanced osteogenic activity.<sup>24,38–40</sup>

In vivo osteogenesis of Si-TiO<sub>2</sub>-NTs, TiO<sub>2</sub>-NTs and Ti screws after insertion into the distal femur of rats were studied. After two and four weeks, the pull-out force of Si-TiO<sub>2</sub>-NTs group increased about 18% and 21% than those of TiO<sub>2</sub>-NTs (Figure 6). By six weeks, the pull-out force showed no significant differences among all the groups. The reason might be that rate of bone formation in rats could be achieved in 28 days, that was much faster than the implants in humans.<sup>41</sup> Further, the values of BV/TV, Tb.Th and Tb.N as well as Tb.Sp of TiO<sub>2</sub>-NTs were significantly higher than Ti screw. Further, the BV/TV and Tb.N of Si-TiO<sub>2</sub>-NTs showed a significant improvement (Figure 7). The results demonstrated that the treatments of nanostructured surface production and silicon implantation had a positive effective effect on implant osseointegration and trabecular microarchitecture formation.

In addition, histological analysis was also performed on the tissue/implant interface to evaluate the bone response on the implants during the healing process. The images showed the bone regeneration capacity of the different screw surfaces (Figure 8). All the three materials (Ti, TiO<sub>2</sub>-NTs and Si-TiO<sub>2</sub>-NTs) exhibited new bone formation within six weeks and newly mineralized trabecular bone was formed between screw threads (green region). Further, a tight and direct bone bonding between the bone and screws modified with Si-TiO<sub>2</sub>-NTs can be observed. In the endosteal region, fluorochrome labels evidenced that a parallel disposition was formed and constituted the internal circumferential lamellae. The similar results of Si-induced bone formation and growth were also observed by others, such as the enhanced longitudinal development of the femur in the Si-OVX group.<sup>42</sup>

## Conclusions

In this work, Si-TiO<sub>2</sub> nanotubes were prepared on the surface of Ti screws. In vitro results show that cells cultured on Si-containing nanotubes exhibited better cell adhesion, proliferation and matrix mineral deposition as well as upregulated expression of osteogenic-related proteins. In vivo osseointegration studies revealed that early-stage new bone formation was promoted on Ti screws modified by Si-TiO<sub>2</sub> nanotubes. These results indicate that the Si-TiO<sub>2</sub>-NTs combining

nanostructure and Si element have the ability to accelerate osseointegration of Ti screws, which would have large potential in improving the properties of Ti implants.

## Acknowledgments

The authors are very grateful to Prof. Xuanyong Liu from Shanghai Institute of Ceramics, Chinese Academy of Sciences for providing the materials and technical assistance for this study. The authors are also grateful to the funding support from National Natural Science Foundation of China (31530024, 31872748), Municipal Health and Family Planning Committee of Wuxi (MS201726), Jiangsu Provincial Special Program of Medical Science (BL2012004), and the Priority Academic Program Development of Jiangsu Higher Education Institutions.

## Disclosure

The authors report no conflicts of interest in this work.

## References

- Long M, Rack HJ. Titanium alloys in total joint replacement—a materials science perspective. *Biomaterials*. 1998;19:1621–1639. doi:10.1016/S0142-9612(97)00146-4
- Wang L, Yang X, Cao WW, et al. Mussel-inspired deposition of copper on titanium for bacterial inhibition and enhanced osseointegration in a periprosthetic infection model. *RSC Adv*. 2017;7:51593–51604. doi:10.1039/C7RA10203H
- Gao CC, Wang Y, Han FX, et al. Antibacterial activity and osseointegration of silver-coated poly (ether ether ketone) prepared using the polydopamine-assisted deposition technique. *J Mater Chem B*. 2017;5:9326–9336. doi:10.1039/C7TB02436C
- Jia L, Han F, Wang H, et al. Polydopamine-assisted surface modification for orthopaedic implants. *J Orthop Transl*. 2019;17:82–95. doi:10.1016/j.jot.2019.04.001
- Lausmaa J, Linder L. Surface spectroscopic characterization of titanium implants after separation from plastic-embedded tissue. *Biomaterials*. 1988;9:277–280. doi:10.1016/0142-9612(88)90098-1
- Albrektsson T, Sennerby L. Direct bone anchorage of oral implants: clinical and experimental considerations of the concept of osseointegration. *Int J Prosthodont*. 1990;3:30–41.
- Chouirfa H, Bouloussa H, Migonney V, Falentin-Daudre C. Review of titanium surface modification techniques and coatings for antibacterial applications. *Acta Biomater*. 2019;83:37–54. doi:10.1016/j.actbio.2018.10.036
- Oh S, Brammer KS, Li YS, et al. Stem cell fate dictated solely by altered nanotube dimension. *P Natl Acad Sci USA*. 2009;106:2130–2135. doi:10.1073/pnas.0813200106
- Zemtsova EG, Yuditceva NM, Morozov PE, Valiev RZ, Smirnov VM, Shevtsov MA. Improved osseointegration properties of hierarchical microtopographic/nanotopographic coatings fabricated on titanium implants. *Int J Nanomed*. 2018;13:2175–2188. doi:10.2147/IJN.S161292
- Sul YT, Johansson CB, Petronis S, et al. Characteristics of the surface oxides on turned and electrochemically oxidized pure titanium implants up to dielectric breakdown: the oxide thickness, micropore configurations, surface roughness, crystal structure and chemical composition. *Biomaterials*. 2002;23:491–501. doi:10.1016/S0142-9612(01)00131-4

11. Variola F, Brunski JB, Orsini G. Nanoscale surface modifications of medically relevant metals: state-of-the art and perspectives. *Nanoscale*. 2011;3:335–353. doi:10.1039/c0nr00485e
12. Oh S, Daraio C, Chen LH, Pisanic TR, Finones RR, Jin S. Significantly accelerated osteoblast cell growth on aligned TiO<sub>2</sub> nanotubes. *J Biomed Mater Res A*. 2006;78:97–103. doi:10.1002/jbm.a.30722
13. Das K, Bose S, Bandyopadhyay A. TiO<sub>2</sub> nanotubes on Ti: influence of nanoscale morphology on bone cell-materials interaction. *J Biomed Mater Res A*. 2009;90:225–237. doi:10.1002/jbm.a.32088
14. Ma Q, Jiang N, Liang S, et al. Functionalization of a clustered TiO<sub>2</sub> nanotubular surface with platelet derived growth factor-BB covalent modification enhances osteogenic differentiation of bone marrow mesenchymal stem cells. *Biomaterials*. 2020;230:119650. doi:10.1016/j.biomaterials.2019.119650
15. Hing KA, Revell PA, Smith N, Buckland T. Effect of silicon level on rate, quality and progression of bone healing within silicate-substituted porous hydroxyapatite scaffolds. *Biomaterials*. 2006;27:5014–5026. doi:10.1016/j.biomaterials.2006.05.039
16. O'Neill E, Awale G, Daneshmandi L, Umerah O, Lo KW. The roles of ions on bone regeneration. *Drug Discov Today*. 2018;23:879–890. doi:10.1016/j.drudis.2018.01.049
17. Xing M, Wang X, Wang E, Gao L, Chang J. Bone tissue engineering strategy based on the synergistic effects of silicon and strontium ions. *Acta Biomater*. 2018;72:381–395. doi:10.1016/j.actbio.2018.03.051
18. Botelho CM, Brooks RA, Best SM, et al. Human osteoblast response to silicon-substituted hydroxyapatite. *J Biomed Mater Res A*. 2006;79:723–730. doi:10.1002/jbm.a.30806
19. Qian S, Liu X. Cytocompatibility of Si-incorporated TiO<sub>2</sub> nanopores films. *Colloids Surf B Biointerfaces*. 2015;133:214–220. doi:10.1016/j.colsurfb.2015.06.007
20. Kermani F, Gharavian A, Mollazadeh S, Kargozar S, Youssefi A, Vahdati Khaki J. Silicon-doped calcium phosphates; the critical effect of synthesis routes on the biological performance. *Mater Sci Eng C-Mater*. 2020;111:110828. doi:10.1016/j.msec.2020.110828
21. Karimi M, Mesgar A, Mohammadi Z. Development of osteogenic chitosan/alginate scaffolds reinforced with silicocarnotite containing apatitic fibers. *Biomed Mater*. 2020;15:055020. doi:10.1088/1748-605x/ab954f
22. Wang Y, Cui W, Zhao X, et al. Bone remodeling-inspired dual delivery electrospun nanofibers for promoting bone regeneration. *Nanoscale*. 2018;11:60–71. doi:10.1039/C8NR07329E
23. Obata A, Tokuda S, Kasuga T. Enhanced in vitro cell activity on silicon-doped vaterite/poly (lactic acid) composites. *Acta Biomater*. 2009;5:57–62. doi:10.1016/j.actbio.2008.08.004
24. Wang T, Qian S, Zha GC, et al. Synergistic effects of titania nanotubes and silicon to enhance the osteogenic activity. *Colloids Surf B Biointerfaces*. 2018;171:419–426. doi:10.1016/j.colsurfb.2018.07.052
25. Zhao X, Wang T, Qian S, Liu X, Sun J, Li B. Silicon-doped titanium dioxide nanotubes promoted bone formation on titanium implants. *Int J Mol Sci*. 2016;17:292. doi:10.3390/ijms17030292
26. Zhang W, Jin Y, Qian S, et al. Vacuum extraction enhances rhPDGF-BB immobilization on nanotubes to improve implant osseointegration in ovariectomized rats. *Nanomed-Nanotechnol*. 2014;10:1809–1818. doi:10.1016/j.nano.2014.07.002
27. Han Y, Chen D, Sun J, Zhang Y, Xu K. UV-enhanced bioactivity and cell response of micro-arc oxidized titania coatings. *Acta Biomater*. 2008;4:1518–1529. doi:10.1016/j.actbio.2008.03.005
28. Yamamoto O, Alvarez K, Kashiwaya Y, Fukuda M. Surface characterization and biological response of carbon-coated oxygen-diffused titanium having different topographical surfaces. *J Mater Sci -Mater M*. 2011;22:977–987. doi:10.1007/s10856-011-4267-x
29. Minagar S, Berndt CC, Wang J, Ivanova E, Wen C. A review of the application of anodization for the fabrication of nanotubes on metal implant surfaces. *Acta Biomater*. 2012;8:2875–2888. doi:10.1016/j.actbio.2012.04.005
30. Torres-Costa V, Martinez-Munoz G, Sanchez-Vaquero V, et al. Engineering of silicon surfaces at the micro- and nanoscales for cell adhesion and migration control. *Int J Nanomed*. 2012;7:623–630. doi:10.2147/IJN.S27745
31. Low SP, Williams KA, Canham LT, Voelcker NH. Evaluation of mammalian cell adhesion on surface-modified porous silicon. *Biomaterials*. 2006;27:43464538. doi:10.1016/j.biomaterials.2006.04.015
32. Qian S, Liu XY, Ding CX. Effect of Si-incorporation on hydrophilicity and bioactivity of titania film. *Surf Coat Technol*. 2013;229:156–161. doi:10.1016/j.surfcoat.2012.07.048
33. Anselme K, Ponche A, Bigerelle M. Relative influence of surface topography and surface chemistry on cell response to bone implant materials. Part 2: biological aspects. *P I Mech Eng H*. 2010;224:1487–1507. doi:10.1243/09544119JEIM901
34. Friguglietti J, Das S, Le P, et al. Novel silicon titanium diboride micropatterned substrates for cellular patterning. *Biomaterials*. 2020;244:119927. doi:10.1016/j.biomaterials.2020.119927
35. Premnath P, Tan B, Venkatakrishnan K. Programming cell fate on bio-functionalized silicon. *Colloids Surf B Biointerfaces*. 2015;128:100–105. doi:10.1016/j.colsurfb.2015.02.013
36. Abazari MF, Hosseini Z, Zare Karizi S, et al. Different osteogenic differentiation potential of mesenchymal stem cells on three different polymeric substrates. *Gene*. 2020;740:144534. doi:10.1016/j.gene.2020.144534
37. Wang Z, Wang X, Tian Y, et al. Degradation and osteogenic induction of a SrHPO<sub>4</sub>-coated Mg-Nd-Zn-Zr alloy intramedullary nail in a rat femoral shaft fracture model. *Biomaterials*. 2020;247:119962. doi:10.1016/j.biomaterials.2020.119962
38. Wang B, Sun JY, Qian S, et al. Adhesion of osteoblast-like cell on silicon-doped TiO<sub>2</sub> film prepared by cathodic arc deposition. *Biotechnol Lett*. 2013;35:975–982. doi:10.1007/s10529-013-1155-0
39. Wang B, Sun J, Qian S, et al. Proliferation and differentiation of osteoblastic cells on silicon-doped TiO<sub>2</sub> film deposited by cathodic arc. *Biomed Pharmacoth*. 2012;66:633–641. doi:10.1016/j.biopha.2012.08.008
40. Zhang Z, Sun J, Hu H, Wang Q, Liu X. Osteoblast-like cell adhesion on porous silicon-incorporated TiO<sub>2</sub> coating prepared by micro-arc oxidation. *J Biomed Mater Res B*. 2011;97:224–234. doi:10.1002/jbm.b.31804
41. Murai K, Takeshita F, Ayukawa Y, Kiyoshima T, Suetsugu T, Tanaka T. Light and electron microscopic studies of bone-titanium interface in the tibiae of young and mature rats. *J Biomed Mater Res*. 1996;30:523–533. doi:10.1002/(SICI)1097-4636(199604)30:4<523::AID-JBM11>3.0.CO;2-I
42. Rico H, Gallego-Lago JL, Hernandez ER, et al. Effect of silicon supplement on osteopenia induced by ovariectomy in rats. *Calcified Tissue Int*. 2000;66:53–55. doi:10.1007/s002230050010

## International Journal of Nanomedicine

Dovepress

### Publish your work in this journal

The International Journal of Nanomedicine is an international, peer-reviewed journal focusing on the application of nanotechnology in diagnostics, therapeutics, and drug delivery systems throughout the biomedical field. This journal is indexed on PubMed Central, MedLine, CAS, SciSearch<sup>®</sup>, Current Contents<sup>®</sup>/Clinical Medicine,

Journal Citation Reports/Science Edition, EMBase, Scopus and the Elsevier Bibliographic databases. The manuscript management system is completely online and includes a very quick and fair peer-review system, which is all easy to use. Visit <http://www.dovepress.com/testimonials.php> to read real quotes from published authors.

Submit your manuscript here: <https://www.dovepress.com/international-journal-of-nanomedicine-journal>